RIPPLE CURRENT REDUCTION BY OPTIMIZING LOAD DEPENDEND SWITCHING LOSSES USING ADAPTIVE CURRENT CONTROL

T.M. Wolbank*, R. Stumberger*, A. Lechner†, J. Machl†

*Department of Electrical Drives and Machines, Vienna University of Technology, A-1040 Vienna, Austria
E-mail: thomas.wolbank@tuwien.ac.at, URL: http://www.tuwien.ac.at
†Schneider Electric Power Drives GmbH, a Company of Schneider Electric, A-1210 Vienna, Austria
E-mail: alois.lechner@schneider-electric.com, URL: http://www.schneider-electric.at

Keywords: Inverter switching frequency, predictive current control, junction temperature, ripple current reduction.

Abstract

In modern inverter fed drive applications the power semiconductors used are typically designed to operate at their maximum thermal operation conditions. Semiconductors worst case thermal considerations in general define the uppermost inverter switching frequency dependent on maximum load current. Fixing this frequency to a constant value, the drive will not be operated with best possible performance at partial load. With the help of the proposed modified predictive current controller it is possible to control both machine current as well as inverter switching frequency at once. Using a thermal model of the power semiconductors hence enables operation at their thermal limit as well as a reduction of current ripple. In a first step the modified predictive current controller as well as the thermal model of the power semiconductors is described. Finally measurement results on a 220kW high precision industrial load dynamometer are presented to compare the performance of a classical predictive current controller and the proposed modification with switching frequency adaptation.

1 Introduction

Not only for industrial high precision drive applications the reduction of ripple current and torque as well as the improved transient current response are of main interest. Increasing inverter switching frequency, in general fulfils both demands at once avoiding computational complex control strategies. On the other hand system components usually have to be operated at least for short durations even above their rated values because of the stringent demand of cost reduction while increasing drive performance. Out of power semiconductors worst case considerations regarding maximum allowable junction temperature the upper limit of the inverter switching frequency can be defined. Fixing this maximum inverter switching frequency to a constant value, conventionally dependent on maximum (over-) load current, the drive will not be operated with best possible performance at partial load.

In modern drive applications PI-controllers in combination with carrier-based pulse width modulation (PWM), are the most widespread solution. Because switching operations are directly linked to the carrier signal, the carrier frequency defines inverter switching frequency, maximum thermal stress of power semiconductors, current controller dead time and hence the transient behaviour of the innermost control loop. Because inverter switching frequency can not be increased arbitrarily for transient response improvement, hysteresis or predictive current control strategies are getting of main interest. Delivering excellent dynamic performance, these approaches on the contrary suffer from a variable inverter switching frequency and high current as well as torque ripple.

2 Modified Predictive Current Controller

As has been shown in previous research, the use of different cost functions within the process of switching state selection of the predictive current controller permits the control of additional state variables such as switching frequency, common mode voltage, or reactive power reduction simultaneously [3], [9]-[13]. However, these cost functions are weighted by a constant factor for defining the importance of the control criteria not able to respond online to variations of the operating point. Introducing a variable weighting factor within the switching state selection and adding it to the predicted current error of each of the possible inverter switching states except the current one, permits the inverter switching frequency to be controlled [1]. The larger the weighting factor gets the more attractive becomes remaining in the current switching state thus decreasing the switching frequency.

The modified quality function for a three phase inverter system providing seven different output voltages (six active and two zero voltage space vectors) therefore can be written according to (1)

$$q_{0..7} = \left| \underline{\Delta i}_{demand} - \underline{\Delta i}_{pred,0..7} \right|^2 + \boldsymbol{A} \cdot k\,, \tag{1}$$

where $\underline{\Delta i}_{demand}$ depicts the demanded current change phasor to exactly match the reference value, $\underline{\Delta i}_{pred,0..7}$ represents the values of the predicted current change phasors caused by each of the possible switching states and k ($k\geq 0$) denotes the penal weight, scaled by one or zero by matrix **A** (zero for the current switching state only).

The inverter switching frequency, proportional to the number of switching transitions per time interval, for the classical predictive current controller (natural inverter switching frequency, $k=0$) as well as for the modified can be calculated with the following assumptions: ideal reactive steady state operation (neglection of stator resistance; assumption of constant load current and speed), initial current deviation is zero and all parameters of the setup are known accurately. For every modulation index m (ratio of back emf magnitude and maximum inverter output voltage) as well as for every penal weight k the resulting inverter switching frequency (scaled to $f_{S,ref}=1/(3T_S)$ where T_S denotes the current controller sampling time), as shown in Fig. 1, can be determined.

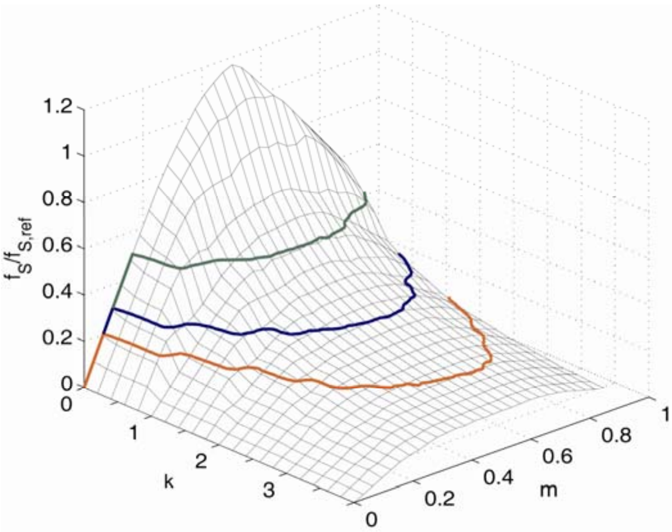

Fig. 1. Simulated predictive current controller inverter switching frequency as a function of modulation index m and the penal weight k (gray); three traces of constant switching frequencies (0.2 – red, 0.3 - blue, 0.5 - green).

2.1 The Switching Frequency Controller

To operate the drive at its thermal limit the inverter switching frequency has to be adjusted dependent on the actual point of operation. For this purpose Fig. 1 shows three traces denoting the correlations between modulation index and penal weight to adjust an almost constant inverter switching frequency (the figure shows the traces for limiting the switching frequency to $f_S/f_{S,ref}=0.2,\ 0.3,$ and 0.5).

The value of the estimated leakage inductance strongly influences the resulting inverter switching frequency (estimated inductance smaller than actual, switching frequency will increase and vice versa). The switching frequency has thus to be controlled in closed loop. For this a switching frequency controller (SFC) was designed which adapts the penal weight k dependent on the actual switching frequency f_S and its demanded value $f_{S,dem}$ (see Fig. 2).

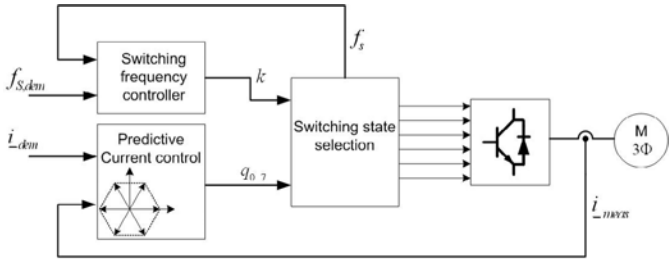

Fig. 2. Block diagram of switching frequency control loop.

2.2 Power Semiconductors Losses and Junction Temperature Modulation

Insulated Gate Bipolar Transistors (IGBT) for the medium power range and switching frequencies up to 100 kHz are getting dominant for modern power electronic actuators [5].

Standard industrial IGBT Voltage-Source Inverter (VSI) systems typically consist of 6 IGBT bridge sections with anti parallel Free-Wheeling Diodes (FWD) respectively. The most relevant parts of semiconductors dissipation are on-state as well as turn-on and turn-of losses. These losses mainly depend on load current and determine device heating. Their magnitudes are generally provided by semiconductor datasheets [6].

For simulation of the junction temperature ϑ_j, which has to be limited to a defined value (typically $\vartheta_{i,max}=150°C$) [6][7], the relevant partial loss components can in a first step be curve-fitted to the characteristics provided by the manufacturer. conduction losses P_{cond} of the IGBT as well as the FWD. They hence can be expressed as:

$$P_{cond} = \left(v_0 + A_{cond} \cdot i_{load}{}^{B_{cond}}\right) \cdot i_{load}\,, \tag{2}$$

where v_0 as well as A_{cond} represent curve-fitting parameters identified from the saturation voltage characteristic (IGBT) and the forward characteristic (FWD) respectively. The value of i_{load} represents the particular load current of the device.

Switching losses are typically depicted as energy losses per switching operation E_{sw} instead of power losses in power semiconductor datasheets. As the mechanisms at turn-on and turn-off of power semiconductors are obeying different physical laws they have to be treated separately. Hence switching losses of the IGBT will be described as $E_{sw,on,IGBT}$ and $E_{sw,off,IGBT}$ whereas for the FWD just energy recovery losses $E_{sw,off,FWD}$ have to be considered.

The exponential approach of the curve-fitting function of the switching losses (IGBT as well as FWD) can hence be expressed as:

$$E_{sw} = A_{0,sw} + \sum_{k=1}^{n} A_{k,sw} \cdot i_{load}{}^{B_{k,sw}}\,, \tag{3}$$

where the index n determines the accuracy of the approximation. $A_{0,sw}$, $A_{k,sw}$ and $B_{k,sw}$ again represent the curve fitting parameters.

To calculate the different device temperatures in a second step, a thermal equivalent circuit can be used describing the relation between IGBTs/FWDs junction temperature as temperature rise due to power losses. Hence mean power dissipations have to be calculated by averaging the switching losses over a defined sampling period (in the presented study the time resolution of dissipation calculation is chosen equal to the current controller sampling time of 10µs). Because of the defined short time duration the device load current i_{load} can be supposed to be constant.

Due to the analogy of the behavior of an electrical capacitor and resistance to their thermal equivalents, power dissipation P_{loss} corresponds to the counterpart current and temperature ϑ to voltage. Consequently thermal equivalent circuits of the power semiconductors and the whole power module can be depicted. Different forms of the model such as "transmission lines", in series connected RC-elements or block diagrams of connected PT1-elements are generally applied [8]. Especially the last mentioned structure is well suited for simulation purposes and is used in this research.
The transient thermal impedance, describing the thermal correlation of junction and case, can hence be expressed as:

$$Z_{th,jc}(t) = \sum_{k=1}^{n} R_{th,k} \cdot \left(1 - e^{\frac{-t}{\tau_{th,k}}}\right), \tag{4}$$

where $\tau_{th,k}=R_{th,k}\cdot C_{th,k}$ represents the thermal time constant of the k-th PT1-element and the number of elements n again determines the accuracy of the approximation. For the present investigation eq. (4) is calculated with n=4 leading to good accuracy in the curve-fitting procedure.

Figure 3 shows a block diagram of the thermal equivalent circuit of a power module. As the thermal impedance $R_{th,ch}$ is equal to both, the IGBT as well as the FWD, both device losses determine the case to heat sink temperature ϑ_{ch}. Furthermore the different instantaneous junction to case temperatures ϑ_{jc} can be calculated with the help of eq. (4) depicted by the dashed boxes in the figure. It only requires an additional thermal sensor at the heat sink to determine the junction temperature being of main interest for worst case thermal design.

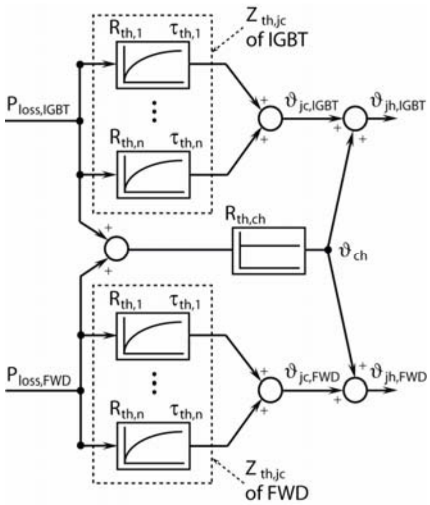

Fig. 3. Block diagram of thermal equivalent circuit of an IGBT and FWD power module.

In addition, Fig. 4 illustrates the simulated junction temperature of phase U upper IGBT and FWD for a particular regenerative load over time. The simulation was performed at a modulation index $m=0.45$. A 100kHz sampling frequency has been used for both, the simulation of the classical predictive current controller (grey temperature traces) and the introduced modified approach (black traces). Using the classical approach, the inverter switching frequency in the investigated point of operation will be approximately 19 kHz. To demonstrate the proposed modified approach, inverter switching frequency will be adjusted to 5 kHz (black temperature traces). When semiconductors load current (upper diagram) is positive it passes the IGBT and dissipation lead to a significant rise of its temperature. The same behavior can be denoted for FWD during negative load current. Their respective junction to case temperature traces ϑ_{jc} are illustrated in the second diagram from top. Assuming a heat sink temperature of $\vartheta_h=80°C$ the lower two diagrams depict absolute junction temperatures ϑ_j of the IGBT and the FWD for the classical as well as the modified approach. Repeatedly exceeding maximum tolerable junction temperature (typically $\vartheta_{i,max}=150°C$) when using classical predictive current control (gray traces) will derogate power semiconductors durability and even may destroy the device.

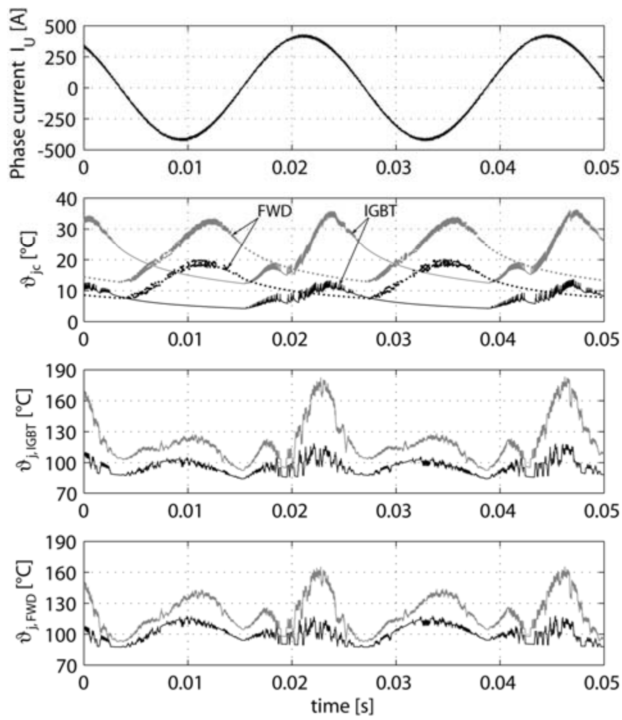

Fig. 4. Simulated junction to case temperature ϑ_{jc} (second from top) and absolute junction temperature ϑ_j of phase U upper IGBT and FWD (lower two diagrams) for 100kHz sampling frequency predictive current control (grey temperature traces: classical approach – natural inverter switching frequency f_s~$19kHz$, black: modified approach – adjusted $f_s=5kHz$). ($\vartheta_h=80°C$, modulation index $m=0.45$)

Without interfering with current controller sampling frequency and its dynamic behavior the modified approach of a switching frequency controller thus permits an adjustment of switching frequency for junction temperature limitation. The maximum junction temperature reached stays well below 125° throughout the period observed.

Figure 4 in addition illustrates IGBTs maximum junction to heat sink temperature $\vartheta_{jh,IGBT}$ of Powerex CM600HA-24A [6] IGBT/FWD module as a function of both, inverter switching frequency f_s and devices load current i_{load}. Calculation of the mentioned differential temperature was performed by simulation of the power semiconductors dissipation and their thermal equivalent circuit described in Fig. 3 with 10µs time resolution. Assuming a heat sink temperature of $\vartheta_h=80°C$, being typical for steady state operation, and a maximum junction temperature of $\vartheta_h=125°C$ for instance, maximum junction to heat sink temperature should not exceed 45°C. To ensure non-destructive power semiconductors operation, maximum load current and inverter switching frequency have to be selected within the dashed area of the lower diagram depicted in Fig. 5.

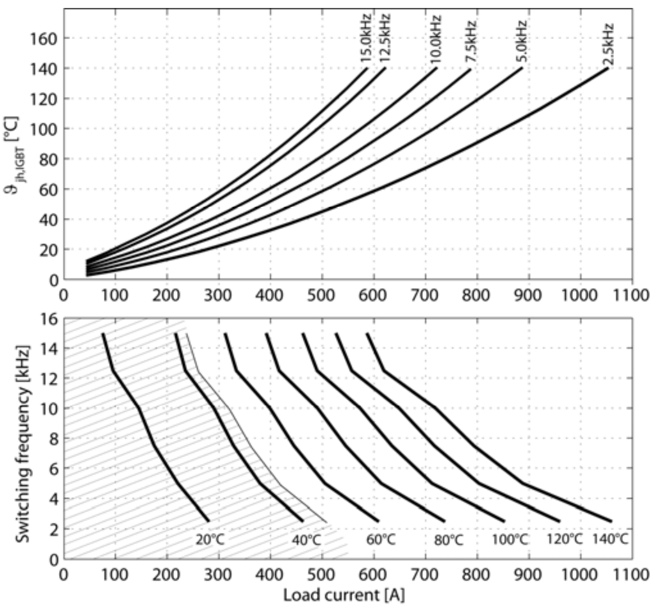

Fig. 5. Simulation of IGBTs maximum junction to heat sink temperature (Powerex CM600HA-24A [6]) of IGBT/FWD as a function of inverter switching frequency and device load current.

It has to be considered, that the characteristics indicated in semiconductor datasheets are based on typical applications. Operating the power semiconductors at their thermal limit hence requires at least additional measurement of the devices turn-on and turn-off behavior on the specific inverter setup. As the application specific gate resistance and Miller capacitance differ from datasheet values, real dissipations can be larger than denoted leading to increased thermal heating of the power semiconductors.

3 Switching Frequency Adaptation for Current Ripple Reduction

Conventional worst-case thermal considerations are used to calculate the upper limit of the inverter switching frequency depending on maximum (over-) load current. Both, load current magnitude and the semiconductors switching frequency, influence device heating. Hence, fixing the inverter switching frequency to a fixed value, as done at conventional carrier-based PWM-methods, the drive will not be operated with best performance at partial load. In addition, when using standard predictive or hysteresis current control, where switching frequency, as well known, is a function of the modulation index, current controller sampling time in general has to be adjusted to limit maximum inverter switching frequency according to the worst-case thermal considerations.
Because of the semiconductors not being operated at their maximum possible switching frequency at partial load (with respect to their thermal limit), the current as well as torque ripple consequently are not optimum.

Using the modified predictive current control with the switching frequency controller hence will reduce current ripple compared to the classical approach twofold:

- *Thermal exploitation of the power semiconductors*
  Figure 6 illustrates the simulated scaled current ripple (vertical axis) as a function of the inverter switching frequency (horizontal axis) for several modulation indices using the modified predictive current controller with a fixed sampling frequency of 100kHz. Obviously even a small switching frequency enhancement can lead to a remarkable reduction of the current ripple.

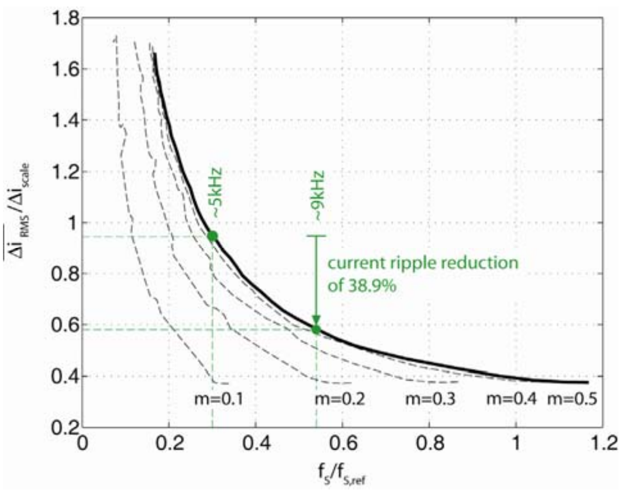

Fig. 6. Simulated current ripple reduction at a modulation index of $m=0.5$ when inverter switching frequency is increased from 5kHz to 9kHz using the modified predictive current controller with a sampling frequency of 100kHz.

When the inverter switching frequency can be increased from 5 to 9kHz (correspond to $f_S/f_{S,ref}=0.2$ to 0.54 for a fixed current controller sampling frequency of 100kHz

depicted in Fig. 6) because of operation at partial load and under consideration of the junction temperature (compare to section *Experimental Results*), the current ripple will decrease by about 39% at $m=0.5$ as depicted in Fig. 6.
For this purpose application specific turn on and turn off behavior of power semiconductors has to be measured for identification of real device dissipations. These data can be used for simulation of the maximum junction temperature, similar to Fig. 5, as a function of inverter switching frequency and load current magnitude. Vertical sections in Fig. 5 consequently mark the functional correlation of inverter switching frequency and load current magnitude in order to keep power dissipations and devices maximum junction temperature below their critical values.

- *Oversampling*
  Using a classical single step predictive discrete time current controller the sampling frequency in general has to be chosen in order to limit maximum inverter switching frequency to a defined value (worst-case thermal design). For reducing current as well as torque ripple switching frequency can be increased. Hence total thermal stress of power semiconductors also increase, making modifications of the inverter cooling system necessary. An alternative approach again is the modified predictive current controller with SFC, decoupling current controller sampling time and inverter switching frequency [2].

To show the effect of oversampling, in Fig. 7 measurement results of the inverter switching frequency as well as the current ripple under no-load operation are depicted using a classical

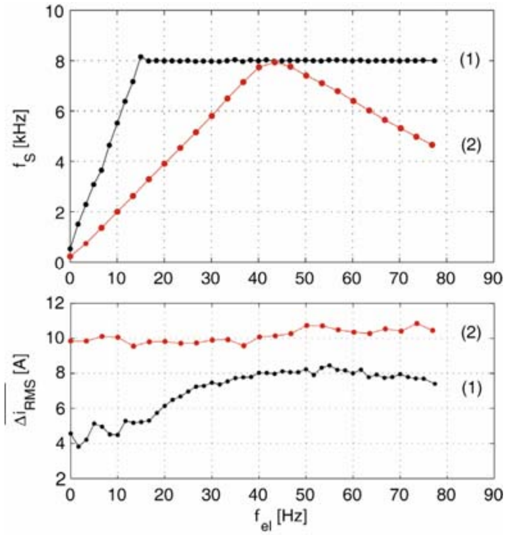

Fig. 7. Measured inverter switching frequency (upper) and ripple current (lower) over motor speed for the classical (2) and the proposed (1) modified predictive current controller with boundary condition of 8kHz max. inverter switching frequency.

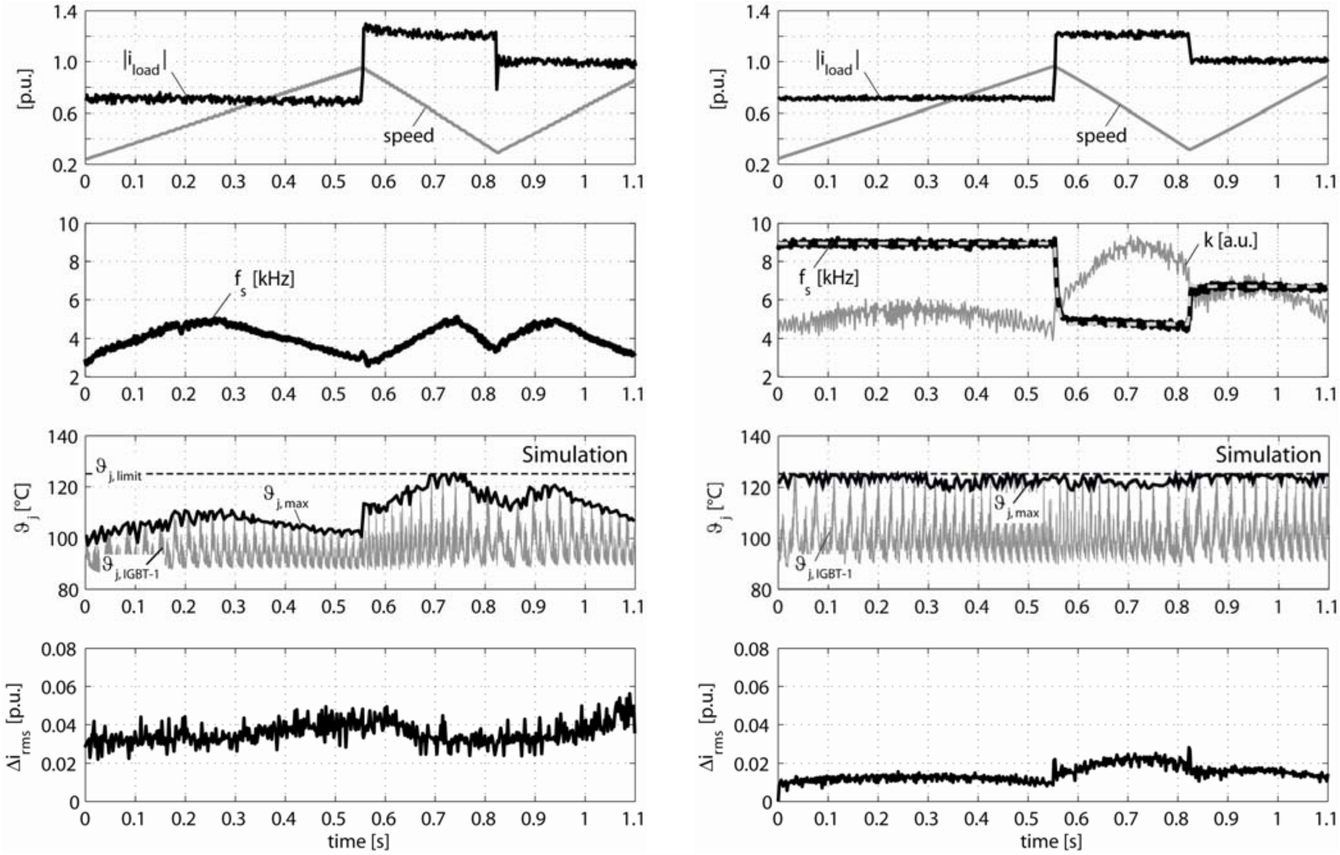

Fig. 8. Measurement of ripple current Δi_{RMS} and simulation of junction temperature ϑ_j using classical predictive current control (left) and the introduced modified approach (right).

predictive current controller (2) and the modified approach (1). To limit thermal stress of the power semiconductors below a critical value, the sampling frequency of (2) has been chosen 25µs to guarantee a maximum inverter switching frequency of about 8kHz. For (1) the sampling time was fixed to 10µs and the reference trace of the switching frequency controller was limited to 8kHz. Although the maximum inverter switching frequency of both approaches are equal, the modified predictive current controller, as can be seen, has a clear advantage in performance with respect to ripple current over the whole speed range.

4 Experimental Results

To verify the proposed method for current ripple reduction by optimum switching frequency adaptation, measurements in combination with junction temperature simulation on an industrial 220kW high precision load dynamometer test stand have been performed (Fig. 8) for classical predictive current control (left), 40µs sampling time has to be used to limit maximum inverter switching frequency and hence maximum junction temperature for the worst case. Using the proposed modified predictive current control (right), allows a sampling time of 10µs because junction temperature limitation is ensured by the switching controller.

As can be seen in the right diagrams of the figure the inverter switching frequency (second from top; actual switching frequency – solid black; demanded – dashed grey) is - dependent on load level and speed (upper diagram) – adjusted by the SFC by varying the penal weight *k (*second diagram from top) to keep maximum junction temperature of all IGBTs and FWDs $\vartheta_{j,max}$ (second from bottom; solid black; temperature trace of one particular IGBT $\vartheta_{j,IGBT-1}$ - grey) just below its defined limit of $\vartheta_{j,limit}=125°C$. Operation with inverter switching frequency close to the thermal maximum by the proposed adaptive current controller hence leads to a clear current and torque ripple reduction especially at partial load (compare the lower diagrams).

5 Conclusions

A novel control strategy for dynamically adjusting inverter switching frequency using a single step predictive current controller was presented. It leads to a remarkable reduction of current as well as torque ripple as the switching frequency can be controlled to always operate the power semiconductors close to their thermal limit. The performance of the proposed strategy is verified by several measurement as well as simulation results.

6 References

[1] T.M. Wolbank, et al., "Strategy for Online Adaptation of Inverter Switching Frequency imposed by a Predictive Current Controller", *IEEE-IEMDC 2009*, pp. 717-723, May 2009.

[2] T.M. Wolbank, R. Stumberger, A. Lechner, J. Machl, "A Novel Control Strategy for Optimal Inverter Switching Frequency Associated with Minimal Current Ripple Using Single Step Predictive Current Control", *Proc. of EPE*, Barcelona, Spain, Sept. 2009.

[3] P. Cortés, et al., "Guidelines for Weighting Factors Design in Model Predictive Control of Power Converters and Drives", *IEEE-ICIT 2009*, pp. 1-7, Feb. 2009

[4] N. Weitendorf, S. Bernet, "Junction Temperature and Switching Frequency Prediction in Direct Torque Controlled Induction Motor Drives", Power Electronics Specialists Conference, IEEE PESC 2008, pp. 338-344, June 2008.

[5] D. Schröder, "Leistungselektronische Bauelemente", Springer-Verlag, Berlin Heidelberg, 2. Auflage, 2006.

[6] Powerex Single IGBTMOD™ A-Series Module (600A/1200V), Datasheet CM600HA-24A, Powerex, Inc., 200 E. Hillis Street, Youngwood, Pennsylvania.

[7] S.A. Kharitonov, M.A. Petrov, D.V. Korobkov, M.A. Maslov, T.Y. Zhoraev, "A Principle of Calculation Dynamic and Static Power Losses with Hard-Switching IGBT", *6th International Siberian Workshop and Tutorials, EDM 2005*, pp. 147-149, July 2005.

[8] V. Blasko, R. Lukaszewski, R. Sladky, "On Line Thermal Model and Thermal Management Strategy of a Three Phase Voltage Source Inverter", *Conf. Rec. IEEE-IAS Annu. Meeting*, Vol. 2, pp. 1423-1431, 1999.

[9] P. Cortés, J. Rodríguez, R. Vargas, U. Ammann, "Cost Function-Based Predictive Control for Power Converters", *IEEE-IECON 2006*, pp. 2268-2273, Nov. 2006.

[10] R. Vargas, P. Cortés, U. Ammann, J. Rodríguez, J. Pontt, "Predictive Control of a Three-Phase Neutral-Point-Clamped Inverter", *IEEE Transactions on Industrial Electronics*, Vol. 54, No. 5, pp. 2697-2705, Oct. 2007

[11] P. Cortés, J. Rodríguez, D.E. Quevedo, C. Silva, "Predictive Current Control Strategy With Imposed Load Current Spectrum", *IEEE Transactions on Power Electronics*, Vol. 23, No. 2, pp. 612-618, March 2008.

[12] R. Vargas, U. Ammann, J. Rodríguez, J. Pontt, "Predictive Strategy to Reduce Common-Mode Voltages on Power Converters", *IEEE-PESC 2008*, pp. 3401-3406, June 2008.

[13] R. Vargas, U. Ammann, J. Rodríguez, J. Pontt, "Reduction of Switching Losses and Increase in Efficiency of Power Converters using Predictive Control", *IEEE-PESC 2008*, pp. 1062-1068, June 2008